

Enriching Tabular Data with Contextual LLM Embeddings: A Comprehensive Ablation Study for Ensemble Classifiers

Gjergji Kasneci
Technical University of Munich
gjergji.kasneci@tum.de
& Enkelejda Kasneci
Technical University of Munich
enkelejda.kasneci@tum.de

November 7, 2024

Abstract

Feature engineering is crucial for optimizing machine learning model performance, particularly in tabular data classification tasks. Leveraging advancements in natural language processing, this study presents a systematic approach to enrich tabular datasets with features derived from large language model embeddings. Through a comprehensive ablation study on diverse datasets, we assess the impact of RoBERTa and GPT-2 embeddings on ensemble classifiers, including Random Forest, XGBoost, and CatBoost. Results indicate that integrating embeddings with traditional numerical and categorical features often enhances predictive performance, especially on datasets with class imbalance or limited features and samples, such as **UCI Adult**, **Heart Disease**, **Titanic**, and **Pima Indian Diabetes**, with improvements particularly notable in XGBoost and CatBoost classifiers. Additionally, feature importance analysis reveals that LLM-derived features frequently rank among the most impactful for the predictions. This study provides a structured approach to embedding-based feature enrichment and illustrates its benefits in ensemble learning for tabular data.

1 Introduction

Feature engineering is foundational to machine learning, playing a critical role in determining the performance, interpretability, and scalability of predictive models. Traditional feature engineering methods rely heavily on domain expertise to transform raw data into representations that meaningfully capture relevant patterns. While effective, this approach is often time-intensive and specific to individual applications, limiting its scalability across diverse tasks. The advent of deep learning, particularly in natural language processing (NLP), has introduced powerful new methods for automated feature extraction. These methods, especially contextual embeddings from models like BERT, RoBERTa, and GPT, can capture rich semantic information from textual data, reducing the need for extensive manual preprocessing and enhancing model robustness across domains [11, 29, 39].

Contextual embeddings offer a valuable means of enhancing tabular datasets by transforming unstructured data into structured, multi-dimensional representations. This transformation has great potential when applied to ensemble classifiers, which have consistently outperformed individual models on a wide range of classification tasks. Ensemble learning methods, such as Random Forest [6], XGBoost [9], and CatBoost [12], combine the strengths of multiple learners, making them highly robust and versatile. Given the state-of-the-art performance of these models, integrating advanced embeddings with traditional tabular features could significantly improve classification accuracy and generalizability, creating a hybrid approach that leverages both structured and unstructured data representations.

Moreover, embeddings can serve as proxies for raw data, addressing challenges related to data and model privacy. In sensitive fields like healthcare, finance, and security, embedding techniques enable the extraction of meaningful insights without exposing identifiable information. This approach aligns with the increasing demand for privacy-preserving machine learning, where both data protection and model interpretability are paramount. By using embeddings to represent raw data, this method allows for privacy-friendly feature engineering that retains the value of the original information while minimizing potential privacy risks.

While prior studies have explored the integration of embeddings within various machine learning architectures, most have focused on specific use cases or single classifiers and often lack a systematic approach across multiple datasets and model types [1, 2, 21, 33, 34]. The effects of embedding-based enrichment on ensemble models across diverse data contexts remain underexplored, leaving a knowledge gap in understanding the generalizability and impact of such techniques. Comprehensive ablation studies, which assess individual contributions of model components, are crucial to address this gap. Ablation analyses can help discern the unique value of embedding-based features relative to baseline features and identify where the combination of embedding and ensemble methods offers the most significant improvements in predictive power.

In this work, we conduct an extensive ablation analysis to assess the impact of embedding-based feature enrichment on ensemble classifiers. Our approach systematically evaluates the integration of embeddings from RoBERTa and GPT-2 into traditional tabular data, comparing performance metrics across several datasets. By examining the performance gains in Random Forest, XGBoost, and CatBoost classifiers, we aim to quantify the benefits of enriched feature representations and provide insights into their contribution to model decisions. Additionally, our feature importance analysis sheds light on the mechanisms and constellations through which contextual embeddings enhance predictive accuracy, thus contributing to a deeper understanding of their role within ensemble learning frameworks. This analysis shows how embedding-based feature enrichment can boost predictive power while also offering a privacy-friendly and efficient approach to modern feature engineering. In summary, this work provides the following contributions:

1. We introduce a generic feature enrichment framework that combines contextual embeddings from LLMs with traditional tabular features.
2. We present a comprehensive ablation study across various benchmark datasets and analyze the performance gains of ensemble classifiers.
3. By examining the top contributing features, we highlight the importance of embedding-based features and provide a deeper understanding of their influence on model predictions.
4. We provide insights into scenarios where embedding-based enrichment is most beneficial, and offer practical guidance on its effective use in classification tasks with structured datasets of

varying complexity.

5. We discuss further potential use cases for embedding-based features, such as privacy-friendly feature representations, reducing reliance on raw, sensitive data without sacrificing predictive power.

The code for this work is open source and available at:
<https://gitlab.lrz.de/rds/featureenrichmentllmembeddings>.

2 Related Work

Feature engineering has been extensively studied, with various approaches proposed to automate and enhance the feature creation process [37, 43, 44]. Traditional methods for feature engineering primarily relied on expert knowledge to craft meaningful representations, but automated feature engineering techniques have emerged to reduce human intervention. Techniques like feature selection, construction, and transformation have been employed to improve model accuracy and interpretability [44]. With the advent of deep learning, feature extraction methods began to incorporate non-linear relationships and hierarchical structures within data, leading to more robust predictive features [3].

The utilization of deep learning models for feature extraction, particularly in NLP, has gained prominence with models like BERT [11], GPT-2 [29], and their successors, which provide contextual embeddings that capture intricate semantic relationships [30, 41]. These models leverage transformer-based architectures [39], which have revolutionized NLP by enabling self-attention mechanisms that learn contextual dependencies within text sequences. More recent models like RoBERTa [23] and GPT-3 [7] have further refined these architectures, leading to embeddings that capture even finer-grained semantic nuances. In domains beyond NLP, embeddings derived from transformers have also been applied to structured data, leading to innovations in feature engineering and transfer learning across heterogeneous data types [5, 10, 13, 17, 19, 21, 27, 40].

Ensemble classifiers have been a staple in machine learning competitions and practical applications due to their robustness and excellent performance on tabular data [4, 6, 9, 12, 15]. These classifiers combine multiple models to improve generalization and reduce variance, with methods like bagging, boosting, and stacking being widely adopted. In recent years, researchers have explored hybrid models that combine traditional ensemble techniques with neural networks to leverage both structured data and unstructured embeddings, yielding significant performance gains [14, 18, 31]. Studies have shown that combining traditional features with deep learning-based embeddings can lead to significant performance gains, especially in domains where feature interactions are complex and multi-modal data is involved [1, 2, 21, 25, 33, 34].

In parallel, approaches for integrating embeddings into ensemble classifiers have been evaluated for their ability to capture hidden patterns within high-dimensional data [1, 2, 45]. For instance, embedding-based feature engineering has proven effective in applications like sentiment analysis, recommendation systems, and medical diagnostics, where context-rich representations enhance model interpretability and predictive power [33, 42]. Recently, methods like knowledge distillation and transfer learning have been employed to integrate pre-trained embeddings, enhancing the adaptability of ensemble classifiers across tasks and datasets [8, 16, 36].

Ablation studies are essential for understanding the contribution of individual components within a machine learning pipeline [20, 24, 35]. They help in identifying which features or components significantly impact the model’s performance, thereby informing feature selection and model

optimization strategies. However, comprehensive ablation analyses that explore the integration of contextual embeddings with ensemble classifiers across diverse datasets remain limited. Prior work has primarily focused on specific use cases or individual classifiers, without a systematic ablation approach to assess the predictive quality of feature subsets across multiple models and datasets [32]. Furthermore, recent advances in explainable AI emphasize the importance of understanding how each feature subset contributes to model predictions, motivating more granular analyses of feature interactions in complex models [22, 26].

This work addresses the above gaps by providing a systematic evaluation of embedding-based feature enrichment in ensemble learning frameworks, thereby contributing to a deeper understanding of feature integration strategies in machine learning. By examining the combined effects of baseline and embedding-enriched features across multiple datasets, this work provides insights into the conditions under which embedding-based feature enrichment enhances model performance, complementing current research in both feature engineering and ensemble learning.

3 Feature Enrichment Framework for LLM Embeddings

Feature enrichment in machine learning involves augmenting the existing feature set with additional features to enhance model performance. This process may integrate both structured and unstructured data sources to enrich the feature space and enable models to capture more complex patterns. In this work, we implement a feature enrichment strategy that combines baseline structured features with embeddings derived from pre-trained language models. To ensure computational efficiency and remain as parsimonious as possible in the enrichment process, we apply Principal Component Analysis (PCA) for initial dimensionality reduction and noise reduction on the embedding dimensions, followed by feature selection to retain only the most informative embedding dimensions.

3.1 General Framework and Definitions

We begin by defining the fundamental concepts and notations used throughout this section.

- Let the **tabular dataset** be represented as $\mathcal{D} = \{(\mathbf{x}_i, y_i)\}_{i=1}^n$, where n is the number of samples. Here, $\mathbf{x}_i \in \mathbb{R}^p$ denotes the feature vector for the i -th sample, and y_i is the corresponding target label.
- The **baseline feature matrix** $\mathbf{X}_{\text{baseline}} \in \mathbb{R}^{n \times p}$ encompasses all original features for each sample in the dataset.
- A set of K **pre-trained language models**, $\mathcal{M} = \{M_1, M_2, \dots, M_K\}$, serves as **feature generators**. For instance, M_1 may correspond to GPT-2, and M_2 to RoBERTa.
- The **transformation function** $\phi : \mathbb{R}^p \rightarrow \mathcal{T}$ converts structured baseline features into textual representations suitable for embedding generation, where \mathcal{T} denotes the space of textual data.
- For each language model $M_k \in \mathcal{M}$, an **embedding function** $f_{M_k} : \mathcal{T} \rightarrow \mathbb{R}^{d_k}$ maps textual input to a d_k -dimensional embedding vector.

3.2 Feature Enrichment Process

The feature enrichment process consists of three primary stages: (1) transformation of structured data into textual format, (2) embedding generation and initial dimensionality reduction using PCA, and (3) feature selection to retain the most informative embedding dimensions.

Stage 1: Transformation to Textual Representation

This stage involves converting structured data into a textual format suitable for input into pre-trained language models [5].

1. For each feature vector $\mathbf{x}_i = [x_{i1}, x_{i2}, \dots, x_{ip}]$, we apply the transformation function ϕ to generate a textual representation:

$$\phi(\mathbf{x}_i) = \text{“Feature1_name: } x_{i1}, \text{ Feature2_name: } x_{i2}, \dots, \text{ FeatureP_name: } x_{ip}\text{”}$$

2. We construct a corpus of textual representations for the entire dataset:

$$\mathbf{X}_{\text{text}} = \{\phi(\mathbf{x}_1), \dots, \phi(\mathbf{x}_n)\}$$

Stage 2: Embedding Generation and PCA Dimensionality Reduction

Given the high dimensionality of embeddings from advanced language models, we apply PCA to remove noise and reduce the embeddings to a manageable size before feature selection.

3. For each language model $M_k \in \mathcal{M}$, we generate an initial embedding matrix $\mathbf{E}_{M_k} \in \mathbb{R}^{n \times D_k}$ by applying the embedding function f_{M_k} to the textual corpus:

$$\mathbf{E}_{M_k} = f_{M_k}(\mathbf{X}_{\text{text}})$$

where D_k is the original embedding dimension (e.g., 768 for GPT-2).

4. We apply PCA to reduce each embedding matrix \mathbf{E}_{M_k} to a lower dimension d (e.g., $d = 50$), resulting in a reduced embedding matrix $\mathbf{E}_{M_k}^{\text{PCA}} \in \mathbb{R}^{n \times d}$:

$$\mathbf{E}_{M_k}^{\text{PCA}} = \text{PCA}(\mathbf{E}_{M_k}, \text{n_components} = d)$$

Stage 3: Feature Selection via Random Forest Importance

To further enhance computational efficiency and focus on the most informative features, we perform feature selection on the PCA-reduced embeddings.

5. We train a Random Forest classifier C_k using $\mathbf{E}_{M_k}^{\text{PCA}}$ to estimate feature importance scores for each embedding dimension.
6. Based on the importance scores, we select the top m most informative dimensions from each $\mathbf{E}_{M_k}^{\text{PCA}}$. Let $\mathcal{J}_{M_k} \subset \{1, \dots, d\}$ denote the indices of these top dimensions. The selected embedding matrix is then:

$$\mathbf{E}_{M_k}^{\text{selected}} = \mathbf{E}_{M_k}^{\text{PCA}}[:, \mathcal{J}_{M_k}]$$

Final Enriched Feature Matrix

We construct the final enriched feature matrix $\mathbf{F}_{\text{enriched}}$ by concatenating the baseline features with the selected embedding dimensions from all language models:

$$\mathbf{F}_{\text{enriched}} = [\mathbf{X}_{\text{baseline}} \mid \mathbf{E}_{M_1}^{\text{selected}} \mid \dots \mid \mathbf{E}_{M_K}^{\text{selected}}]$$

This comprehensive approach ensures that we integrate rich contextual information from language models while maintaining computational tractability and model interpretability.

4 Methodology for Classifier Evaluation and Ablation Study

This section presents the methodological framework used to assess the efficacy of embedding-based feature enrichment in enhancing ensemble classifiers. We detail the processes of dataset preparation, feature enrichment, classifier training, ablation study design, evaluation metrics, and statistical validation to ensure the robustness and reproducibility of our findings.

4.1 Experimental Setup

In the following, we describe the experimental setup developed to accurately evaluate the effects of embedding-based feature enrichment on classification performance. This approach encompasses dataset selection, preprocessing, feature engineering, and classification model configuration to ensure a systematic and reproducible evaluation process.

Table 1: Comprehensive Overview of Datasets Used in the Study

Dataset	Classes	Instances	Tot. Feat.	Cat. Feat.	Num. Feat.	Class Dist.	Miss. Vals.	Source
UCI Adult	2	65,123	14	8	6	24% >\$50K, 76% ≤\$50K	Yes	UCI
UCI Heart Disease	2	303	13	5	8	54% No Disease, 46% Disease	Yes	UCI
UCI Wine Quality	10	1,599	11	0	11	Varies Across 10 Classes	No	UCI
Titanic	2	1,309	12	3	4	38% Survived, 62% Not Survived	Yes	Kaggle
Pima Indians Diabetes	2	768	8	0	8	35% Positive, 65% Negative	No	UCI
Breast Cancer Wisconsin	2	569	30	0	30	63% Benign, 37% Malignant	No	UCI
Car Evaluation	4	1,728	6	6	0	70% Unacc., 22% Acc., 4% Good, 4% Vgood	No	UCI
UCI Letter Recognition	26	20,000	17	0	16	Approximately Uniform	No	UCI
UCI Covertypes*	7	581,012	54	44	10	Varies Across 7 Classes	No	UCI

Datasets. To ensure the generalizability of our results across diverse domains, we utilized ten benchmark datasets of varying sizes and complexities (in terms of features and instances) from the UCI Machine Learning Repository¹ and Kaggle². The selected datasets encompass binary and multi-class classification tasks with differing types and numbers of features and instances. Table 1 provides a comprehensive overview of the relevant aspects of these datasets.

¹<https://archive.ics.uci.edu/>

²<https://www.kaggle.com/datasets>

*Except for the UCI `Coverttype` dataset – where 15% of the data was used, sampled through stratified sampling – all other datasets were used in their full form.

Data Preprocessing. Each dataset underwent careful and rigorous preprocessing to ensure data quality and suitability for analysis:

- **Handling Missing Values:** Missing values in categorical features were imputed using the mode while missing numerical values were imputed with the mean. Rows with missing target values (i.e., class labels) were dropped.
- **Encoding Categorical Variables:** One-Hot Encoding was utilized for nominal categorical variables, transforming them into binary vectors.
- **Feature Scaling:** Numerical features were standardized using the *StandardScaler* to ensure zero mean and unit variance.
- **Target Variable Encoding:**
 - For **binary classification** tasks, target labels were mapped to 0 and 1.
 - For **multi-class classification** tasks, the target variable was encoded using *LabelEncoder*.

4.2 Feature Engineering and Enrichment

Embedding Generation and Dimensionality Reduction. We generated contextual embeddings using two pre-trained language models, namely RoBERTa and GPT-2. The embedding generation and dimensionality reduction process is formalized in three steps as follows:

1. The step of **textual transformation**, where the following transformation is applied to each instance \mathbf{x}_i :

$$\phi(\mathbf{x}_i) = \text{Concatenate}(\{f_j : v_{ij}\}_{j=1}^p)$$

where f_j are feature names and v_{ij} are feature values.

2. The step of **embedding generation**, where, for each pre-trained language model M_k , we map the textual representation of the tabular dataset into the embedding space to obtain the corresponding embedding matrix:

$$\mathbf{X}_{\text{text}} = \{\phi(\mathbf{x}_1), \dots, \phi(\mathbf{x}_n)\}$$

$$\mathbf{E}_{M_k} = f_{M_k}(\mathbf{X}_{\text{text}})$$

where f_{M_k} is the embedding function for model M_k .

3. The step of noise removal through **PCA-based dimensionality reduction**:

$$\mathbf{E}_{M_k}^{\text{PCA}} = \text{PCA}(\mathbf{E}_{M_k}, \text{n_components} = d)$$

with $d = 50$ to still have a high coverage of relevant dimensions.

Feature Selection. We employed Random Forest feature importance to select and retain the most informative embedding dimensions:

1. We conduct a **feature importance estimation** by applying a Random Forest classifier C_k to $\mathbf{E}_{M_k}^{\text{PCA}}$. Specifically, we train C_k on $\mathbf{E}_{M_k}^{\text{PCA}}$ to obtain importance scores.
2. Then we **select the top features** based on the computed importance score as:

$$\mathbf{E}_{M_k}^{\text{selected}} = \mathbf{E}_{M_k}^{\text{PCA}}[:, \mathcal{J}_{M_k}]$$

where \mathcal{J}_{M_k} are indices of the top $m = 10$ features. Importantly, our analysis tested different numbers of features from the PCA-reduced embeddings. We found that selecting the top 10 features captured all the relevant information for the classification tasks. This approach remained efficient and parsimonious, balancing accuracy with simplicity.

4.3 Classifier Selection and Training

Classifiers. We used three ensemble classifiers, each known for robustness and strong performance on tabular data [4]:

1. **Random Forest Classifier** [6]: An ensemble of decision trees utilizing bagging to improve generalization and reduce overfitting.
2. **XGBoost Classifier** [9]: An optimized gradient boosting framework known for its efficiency and high performance.
3. **CatBoost Classifier** [12]: A gradient boosting library that inherently handles categorical features and employs ordered boosting to mitigate overfitting.

Hyperparameter settings. In this study, classifiers were configured with consistent hyperparameters across all feature subsets and datasets to attribute performance improvements directly to the impact of embedding-based feature enrichment rather than model-specific tuning. By standardizing these settings, we ensure a fair comparison that isolates the contributions of enriched features, highlighting their intrinsic value in boosting model accuracy and feature importance. For this purpose, we used the following hyperparameters: Random Forest with 100 estimators and balanced class weights; XGBoost with default tree depth, learning rate of 0.1, and ‘mlogloss’ as the evaluation metric; and CatBoost with default parameters and a random seed for reproducibility.

4.4 Ablation Study Design

To thoroughly assess the contribution of embedding-based feature enrichment, we designed a structured ablation study that isolates the effects of various feature subsets on classifier performance. This approach enables a clear comparison between models with baseline features and those enhanced by RoBERTa and GPT-2 embeddings, quantifying their impact on predictive accuracy.

Feature Subset Definitions. For our ablation study, we defined the following feature subsets to pinpoint which combinations of baseline and embedding features yield the highest predictive value:

1. **Baseline:** Original preprocessed features.
2. **GPT2_Selected:** Selected GPT-2 embedding features.
3. **RoBERTa_Selected:** Selected RoBERTa embedding features.
4. **Baseline_GPT2_Selected:** Baseline features with selected GPT-2 embeddings.
5. **Baseline_RoBERTa_Selected:** Baseline features with selected RoBERTa embeddings.
6. **GPT2_RoBERTa_Selected:** Combined selected embeddings from both models.
7. **Baseline_GPT2_RoBERTa_Selected:** Baseline features with selected embeddings from both models.

Evaluation Strategy for the Ablation Study. The ablation study evaluates the performance of the classifiers on the above feature subsets with the goal to assess the contribution of embedding-based features. For each dataset and classifier:

1. For the validation of the models, we perform a stratified **5-fold cross-validation** is performed. Specifically, each classifier is trained on the training folds for each feature subset.
2. Relevant **classification performance metrics** such as Accuracy, Balanced Accuracy, Weighted F1 Score, and ROC-AUC are computed on the validation fold.
3. **Paired t-tests** compare performance across feature subsets.

Algorithmic Procedure. For clarity and reproducibility, the ablation study procedure is encapsulated in Algorithm 1. It outlines each step of our approach for evaluating feature subset contributions to classifier performance.

In addition to the robust and systematic preprocessing, feature subset selection, and embedding pipeline, Algorithm 1 employs stratified cross-validation and paired statistical testing to provide robust, comparative insights into the predictive power of enriched features. This modular, step-by-step approach enables the systematic isolation of feature subset effects, enhancing the interpretability and precision of the ablation study’s results. Figure 1 depicts the pipeline used in the study.

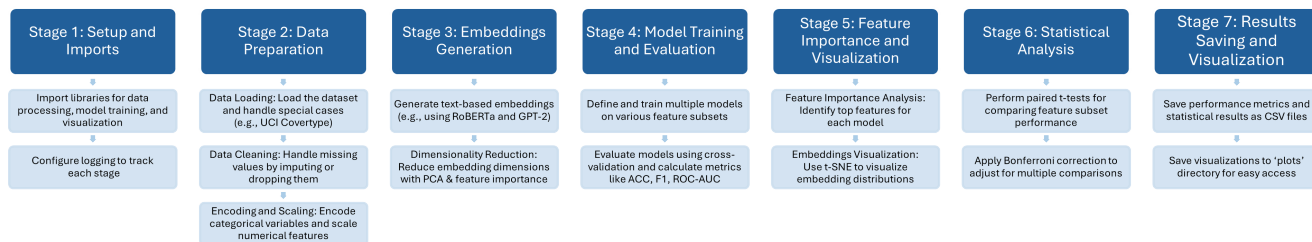


Figure 1: Overview of the experimental workflow stages.

Algorithm 1 Ablation Study Procedure

Require: Dataset D , Feature Subsets \mathcal{F} , Classifiers \mathcal{C}

```
1: for each dataset  $D \in \mathcal{D}$  do
2:   Preprocess dataset  $D$ 
3:   Encode categorical variables and scale and normalize numerical features
4:   Generate textual representations from  $D$ 
5:   Create embeddings using transformer models (e.g., RoBERTa, GPT-2)
6:   Apply PCA to reduce embedding dimensions to  $d = 50$ 
7:   Select top-10 features based on feature importance and apply t-SNE for 2D visualization
8:   for each classifier  $C \in \mathcal{C}$  do
9:     for each feature subset  $F \in \mathcal{F}$  do
10:      Initialize lists to store Accuracy, Balanced Accuracy, Weighted F1 Score, ROC-AUC
11:      Create 5 stratified folds for cross-validation from dataset  $D$ 
12:      for fold  $k = 1$  to 5 do
13:        Define fold  $k$  as the validation set  $(X_{\text{val}}^k, y_{\text{val}}^k)$ 
14:        Define the remaining folds as the training set  $(X_{\text{train}}^k, y_{\text{train}}^k)$ 
15:        Train classifier  $C$  on  $X_{\text{train}}^k, y_{\text{train}}^k$  using features from subset  $F$ 
16:        Predict labels  $\hat{y}^k$  using  $C$  on  $X_{\text{val}}^k$ 
17:        Compute Accuracy, Balanced Accuracy, Weighted F1 Score, ROC-AUC
18:        Record the computed metrics for fold  $k$ 
19:      end for
20:      Compute average of each metric over the 5 folds for classifier  $C$  and feature subset  $F$ 
21:      Analyze feature importance using classifier  $C$  on subset  $F$ 
22:      Select top-10 most important features based on feature importance scores
23:      Save results for metrics, feature importance
24:    end for
25:    Perform paired t-tests to compare metrics across feature subsets  $\mathcal{F}$  for  $C$  and save results
26:  end for
27: end for
```

4.5 Evaluation Metrics

To comprehensively assess classifier performance and capture various aspects of predictive accuracy, we employed multiple evaluation metrics, ensuring a robust and nuanced evaluation:

- We use **Accuracy** and **Balanced Accuracy** to assess general performance and the ability to handle class imbalance, respectively:

$$\text{Accuracy} = \frac{1}{n} \sum_{i=1}^n \mathbf{1}\{\hat{y}_i = y_i\}$$

where n is the total number of instances, \hat{y}_i is the predicted label, and y_i is the true label for instance i .

$$\text{Balanced Accuracy} = \frac{1}{C} \sum_{c=1}^C \frac{\text{TP}_c}{\text{TP}_c + \text{FN}_c}$$

where C is the number of classes, TP_c and FN_c are the true positives and false negatives for class c , respectively. Balanced Accuracy accounts for class imbalance by averaging recall over all classes.

- To analyze the precision and recall-based performance, we include the **weighted F1 score**, which is particularly important in datasets with class imbalance:

$$\text{Weighted F1 Score} = \sum_{c=1}^C \frac{N_c}{N} \cdot \text{F1 Score}_c$$

where N_c is the number of true instances in class c , N is the total number of instances, and F1 Score_c is the F1 Score for class c . The F1 Score for each class is calculated as:

$$\text{F1 Score}_c = 2 \cdot \frac{\text{Precision}_c \cdot \text{Recall}_c}{\text{Precision}_c + \text{Recall}_c}$$

with precision and recall defined for each class.

- To analyze the discriminative performance through a threshold-independent performance measure, we employ **ROC-AUC**:

$$\text{ROC-AUC} = \int_0^1 \text{TPR}(FPR^{-1}(t)) dt$$

For multi-class classification, we use the macro-averaged ROC-AUC computed using the One-vs-Rest approach. In addition, all ROC curves were plotted for visual assessment and comparisons.

- For fine-granular per-class performance analysis, we generate a **classification report** with detailed per-class metrics, including all the metrics and the paired t-test introduced above.

4.6 Statistical Significance Testing

Paired t-tests were conducted between all pairs of feature subsets for each classifier and dataset combination. The **Bonferroni correction** was applied to adjust for multiple comparisons, ensuring thus a family-wise significance level of $\alpha = 0.05$, which overall is way more conservative than using $\alpha = 0.05$ for each pair-wise comparison.

4.7 Implementation Details

All experiments were implemented in Python 3.8, leveraging the following libraries:

- **scikit-learn** [28] was used for data preprocessing, model training, evaluation metrics, PCA, and feature selection.
- **XGBoost** [9] and **CatBoost** [12] were employed for the respective classifiers.
- **Hugging Face Transformers** [41] facilitated the generation of contextual embeddings using pre-trained RoBERTa and GPT-2 models.

- **Matplotlib** and **Seaborn** were utilized for data visualization, including feature importance plots and ROC curves.

The Experiments were conducted on a machine equipped with an Intel Core i7 processor, 32 GB RAM, and an NVIDIA GeForce RTX 4050 GPU. GPU acceleration was utilized for embedding generation to expedite processing times. Additionally, all software dependencies were managed using `conda` environments to ensure reproducibility.

We encountered several practical challenges during the experiments, necessitating strategies to address memory management, processing efficiency, and reproducibility, as outlined below:

- **Memory management** can be challenging when handling large datasets with high-dimensional embeddings. To mitigate memory issues and avoid crashes, we implemented all relevant data-processing steps as batch-wise processing.
- The **processing time** can also be an issue when generating embeddings for large datasets; therefore, in addition to batch processing, we leveraged vectorized operations with libraries like NumPy and Pandas.
- For **reproducibility** purposes and to ensure our results were consistent across different runs, we set fixed random seeds for all libraries involved in stochastic processes. This included setting seeds to a fixed value for NumPy, TensorFlow, PyTorch, and the random module.

5 Performance Evaluation

This section presents the results of our evaluation of embedding-based feature enrichment on ensemble learning classifiers, specifically Random Forest, XGBoost, and CatBoost, across the eight benchmark datasets presented in Table 1. Based on a detailed ablation study, we evaluated the effects of combining traditional features with embeddings from pre-trained language models, specifically RoBERTa and GPT-2. All results are presented in this section, with further details in the Appendix, Table 2. The integration of these contextual embeddings demonstrated significant improvements in predictive performance, particularly in datasets with limited representativeness, i.e., imbalanced datasets or datasets with limited features or samples.

5.1 Overall Performance Trends Across Models and Feature Subsets

Performance Trends. As shown in Figure 2, in many datasets, feature subsets that incorporate embeddings show clear improvements in both Weighted/Balanced Accuracy, F1, and ROC-AUC Score over the baseline features alone. For example, in the `UCI Adult`, `Pima Indian Diabetes`, `Titanic` and `Heart Disease` datasets, feature subsets enhanced with GPT-2 and RoBERTa embeddings yield significant gains, especially in combinations with more advanced ensemble classifiers, such as XGBoost and CatBoost. These results suggest that the embedding-based enrichments capture essential information that improve classification. Moreover, XGBoost and CatBoost benefit from the enriched features more often than the Random Forest classifier. This can also be seen in Figure 3, which shows the absolute counts of wins per classifier, per feature subset.

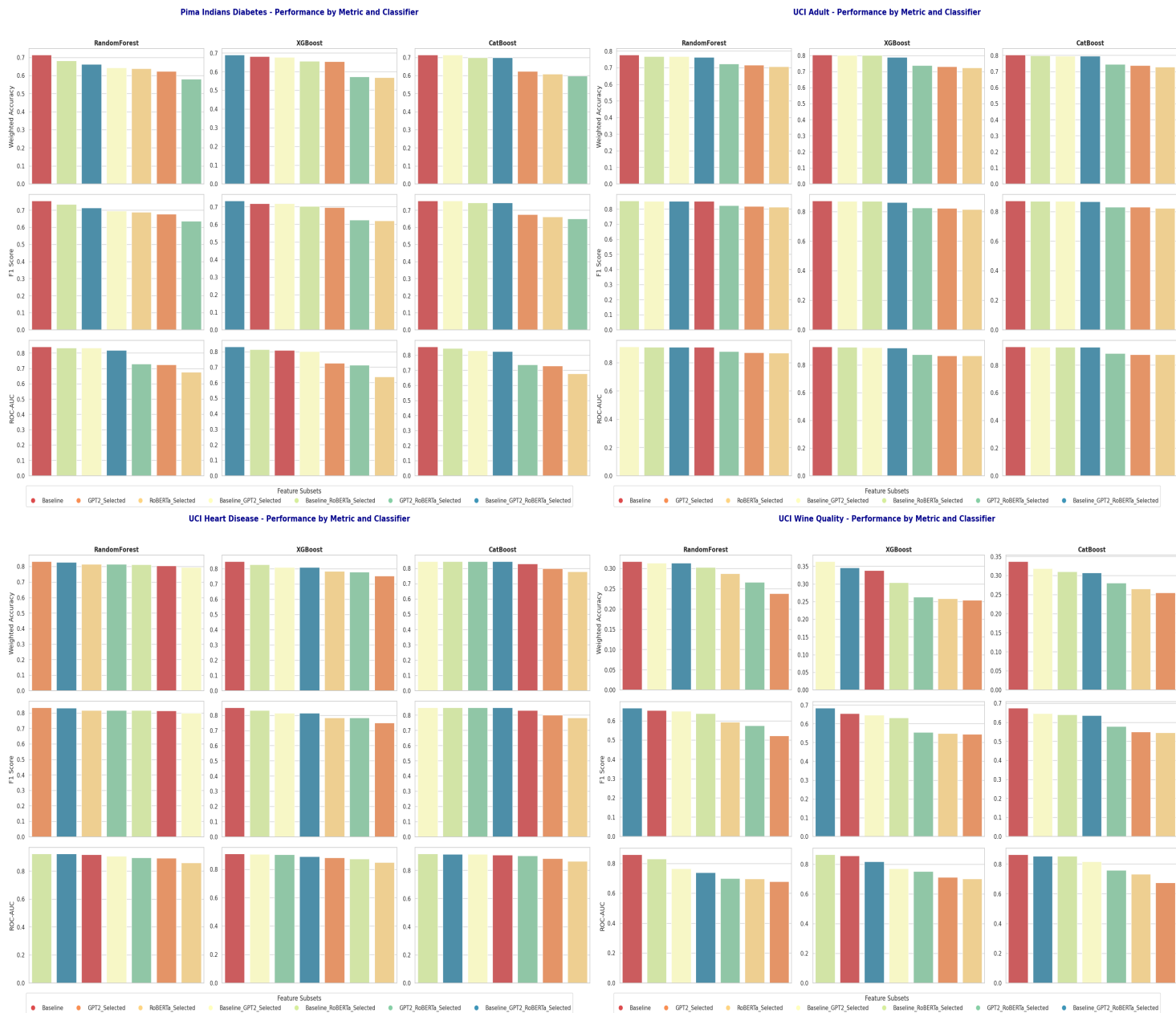


Figure 2: Performance metrics (Weighted/Balanced Accuracy, F1 Score, and ROC-AUC) for different feature subsets on multiple datasets (Pima Indians Diabetes, UCI Adult, UCI Heart Disease, and UCI Wine Quality) using Random Forest, XGBoost, and CatBoost classifiers. Each plot shows how different feature subsets influence classifier performance, with results sorted by feature subset to facilitate comparisons.

Key Takeaways. A key insight from these results is that for datasets with limited representativeness – such as those found in medical applications – the computational overhead in embedding-based feature enrichment can be well justified by the performance gains achieved. Embeddings add valuable semantic context, compensating for the scarcity of features or class diversity, and thus can enhance model performance. The gains from the embedding-derived features can be further amplified with more advanced ensemble classifiers such as XGBoost or CatBoost.

Conversely, for datasets with robust representation across classes and features, the benefits of embedding enrichment tend to be marginal at best, as these datasets already offer sufficient information for the model to learn effectively.

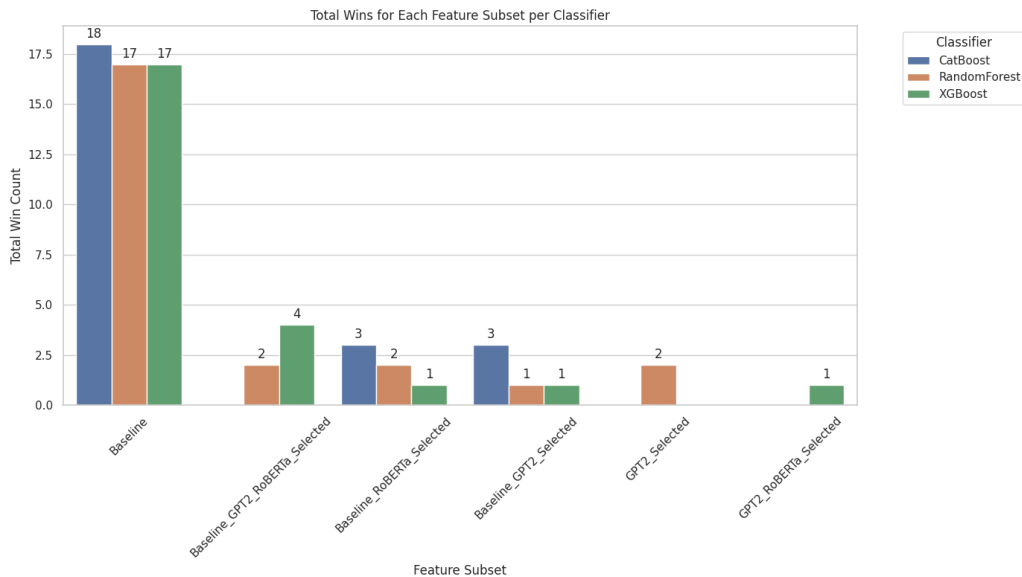


Figure 3: Total wins for each feature subset per classifier.

5.2 Statistical Significance of Performance Improvements

To assess whether the integration of contextual embeddings (i.e., GPT-2 and RoBERTa) yields significant improvements in model performance compared to baseline features, we conducted a series of Bonferroni-corrected paired t-tests across all classifiers and datasets used in this study. These t-tests compared different feature subsets to determine if embedding-based enrichments had a statistically significant effect ($p < 0.05$) on metrics such as accuracy, balanced accuracy, F1 score, and ROC-AUC.

Figures 10, 11, and 12 from the Appendix illustrate pairwise statistical significance analyses among feature subsets across the eight benchmark datasets. Each subplot shows a matrix of pairwise comparisons, where the value of 1 in dark-colored cells indicates that the differences between feature subsets are statistically significant ($p < 0.05$, after Bonferroni correction).

In comparison to subsets involving only baseline features, we often found significant performance enhancements in feature subsets enriched with GPT-2 and RoBERTa embeddings, mostly in combination with XGBoost and CatBoost. However, the performance gains were varied, which suggests that while contextual embeddings may offer benefits for the predictive performance, the extent of those benefits may depend on dataset characteristics such as class representation and balance, dataset complexity, and feature diversity. For the UCI **Letter Recognition** and **Covertypes** datasets, we did not observe any gains from embedding-derived features, no matter which classifier or which enriched feature subset was used. We hypothesize that these two datasets already possess highly informative and well-defined feature sets that effectively capture the underlying patterns needed for classification. When datasets are structured and have robust representations, embeddings may not add significant value, as the original features alone suffice for accurate predictions.

5.3 Feature Importance Analysis

In order to understand the relative impact of different feature subsets on model predictions, we conducted an extensive feature importance analysis, with importance scores derived from the Random Forest, XGBoost, and CatBoost classifiers. Figures 4, 5, and 6 present the top 10 features for the three best-performing feature subsets across three selected datasets, namely the UCI **Adult**, **Pima Indians Diabetes**, and **Heart Disease**.

Across classifiers and datasets, embedding-derived features, such as those from GPT-2 and RoBERTa, frequently rank among the most important, which illustrates their significant contribution to classification outcomes. For example, in Figure 4, GPT-2 and RoBERTa features appear prominently among the top-10-ranked features for the UCI **Adult** dataset, indicating that these embeddings effectively capture essential information that complements the original tabular features.

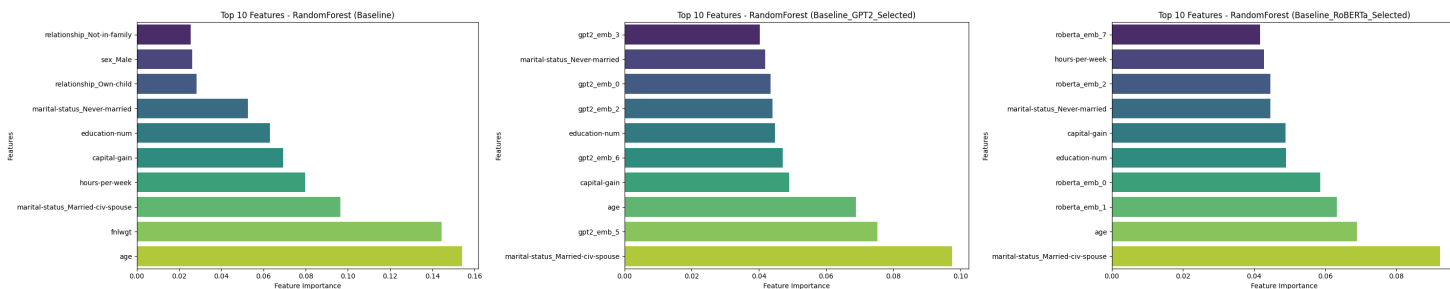


Figure 4: Random Forest top-10 features for the three best performing feature subsets on the UCI **Adult** dataset.

In the case of the **Pima Indians Diabetes** dataset, as shown in Figure 5, the XGBoost classifier reveals a similar trend where embedding-based features contribute to the model’s output beyond the capacity of baseline features alone. This underscores the impact of contextual embeddings in enriched feature subsets.

For the UCI **Heart Disease** dataset, Figure 6 highlights the impact of embedding-enriched features using the CatBoost classifier. For this dataset, the combination of baseline features and embeddings provides a richer representation. However, interestingly, the CatBoost classifier performed best on the combination features derived from GPT-2 and RoBERTa embeddings alone.

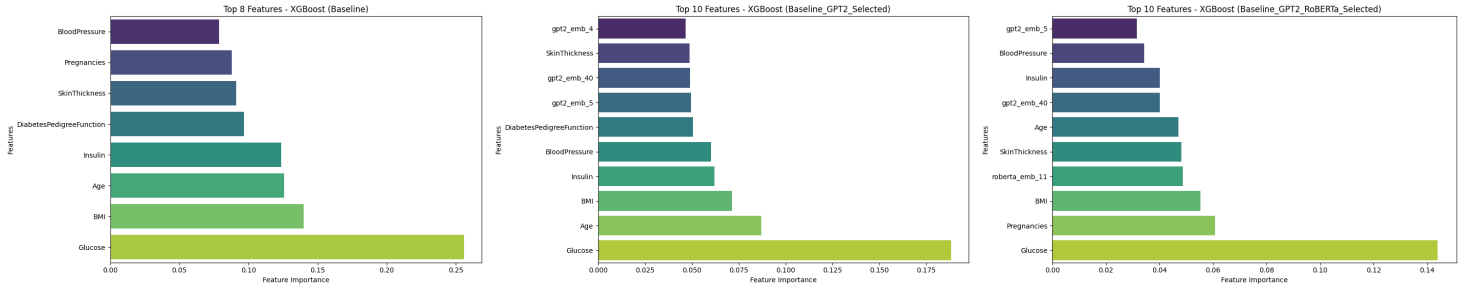


Figure 5: XGBoost top-10 features for the three best-performing feature subsets on the UCI Pima Indian Diabetes dataset.

This suggests that the embeddings effectively capture medically relevant information that the original features might miss.

As showcased by these examples, embeddings generated from pretrained LLMs may provide a complementary view by incorporating additional semantic information and lead to improved decision-making by ensemble classifiers. The consistent presence of these features among the top ranks suggests that their integration is deemed important by the underlying model and might help enhance representation diversity.

We believe that such hybrid approaches have the potential to advance feature engineering practices, especially in ensemble learning frameworks, by leveraging the strengths of both feature types to improve predictive performance and generalizability.

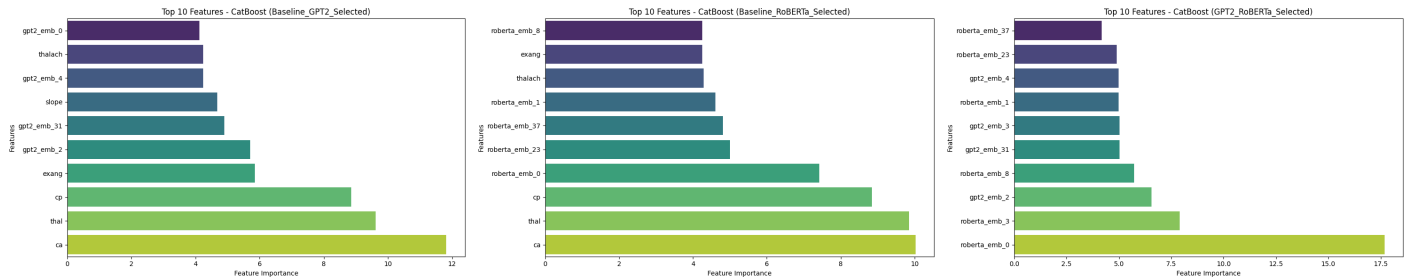


Figure 6: CatBoost top-10 features for the three best performing feature subsets on the UCI Heart Disease dataset.

5.4 Visualization of Embedding Distributions

To further illustrate the discriminative power of the generated embeddings, we employed t-distributed Stochastic Neighbor Embedding (t-SNE) [38] to project high-dimensional embedding vectors into a 2D space. Figures 7 and 8 depict the clustering of RoBERTa and GPT-2 embeddings with respect to target classes in the UCI Adult and UCI Heart Disease datasets, respectively.

These visualizations reveal clustering patterns corresponding to different target classes, affirming that the embeddings encapsulate discriminative information conducive to accurate classification.

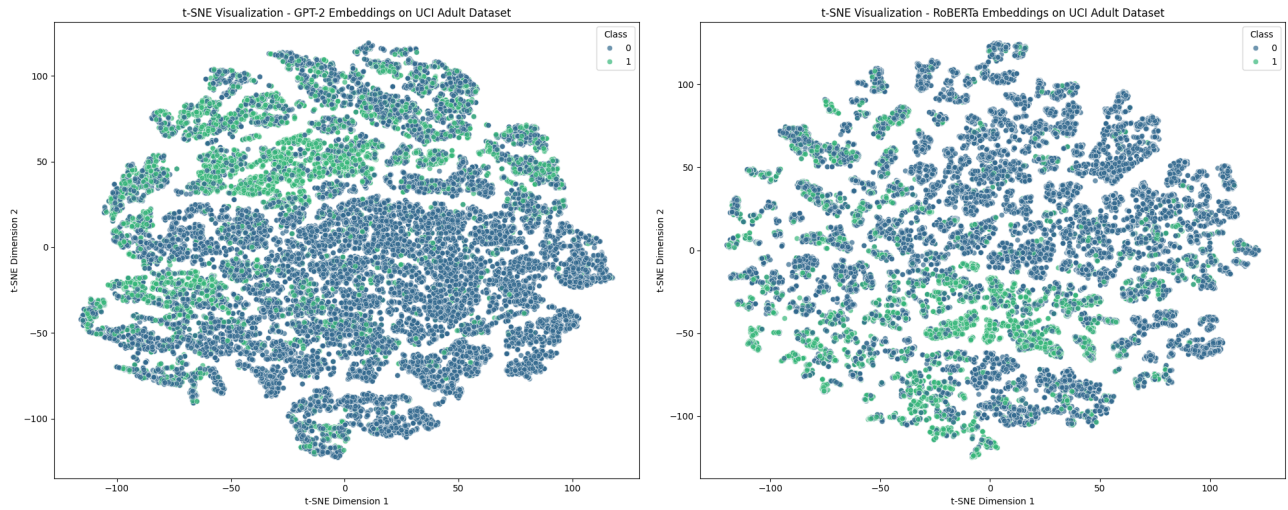


Figure 7: t-SNE applied to the selected GPT-2 and RoBERTa embeddings from the UCI Adult dataset for 2D visualization.

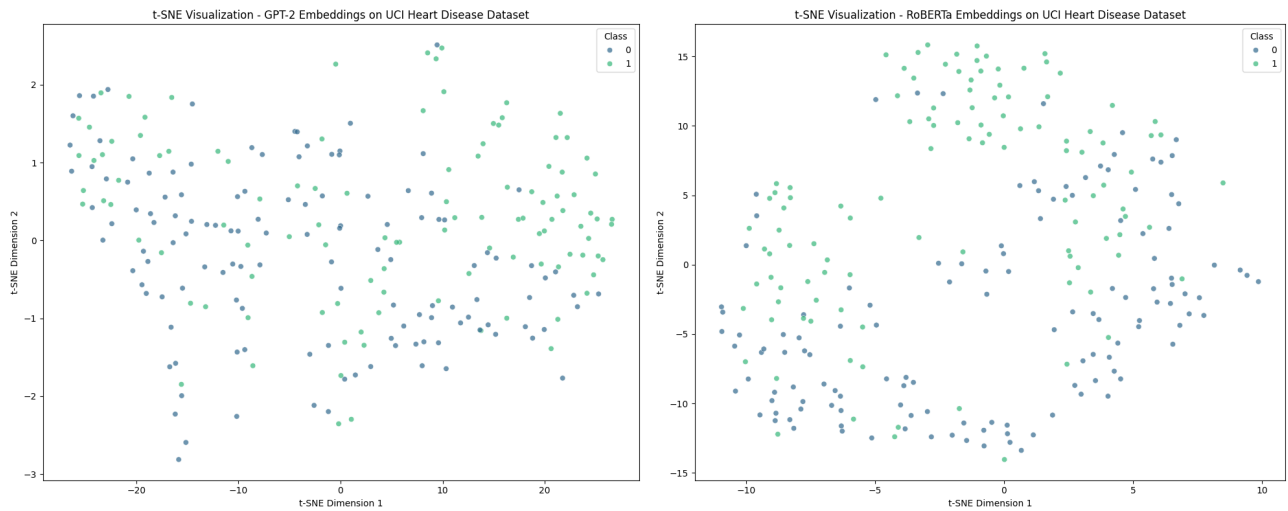


Figure 8: t-SNE applied to the selected GPT-2 and RoBERTa embeddings from the UCI Heart Disease dataset for 2D visualization.

6 Discussion

6.1 Privacy-Preserving Potential of Embeddings

Privacy Advantages of Embedding-Based Representations. Embedding-based features present an effective approach to privacy-preserving machine learning, particularly beneficial in do-

mains like healthcare. By abstracting raw data into high-dimensional embeddings, sensitive details are veiled, reducing the risk of data exposure. Embedding-only subsets, such as GPT2_Selected and RoBERTa_Selected, often perform well, slightly worse than raw-feature-based models. They align well with privacy-by-design principles and regulatory standards like GDPR and allow for acceptable predictive performance without direct reliance on sensitive features, offering both compliance and robust data protection.

Transferability and Model Privacy. Leveraging embeddings from pre-trained models like GPT-2 and RoBERTa enhances model flexibility and transferability. These embeddings encapsulate generalizable patterns that protect specific dataset characteristics, enabling safe, effective deployment across applications. By allowing organizations to reuse these representations without exposing unique dataset details, embedding-based enrichment meets both the privacy and versatility needs of modern machine learning workflows.

Regulatory Alignment and Data Minimization. Embedding-based feature enrichment aligns well with data minimization principles by reducing the model’s dependency on raw, sensitive data. This approach lowers the need for ongoing access to personal information, supporting compliance with privacy regulations without sacrificing model quality. Embedding transformations, which enhance both performance and data protection, represent a new paradigm where privacy preservation complements predictive accuracy, setting a high standard for ethical AI.

6.2 Limitations

The proposed method faces several limitations. First, embeddings from pretrained LLMs like GPT-2 and RoBERTa generate computational overhead, posing scalability challenges for large datasets or real-time applications. The use of 50 PCA components and selecting the top 10 features were based on preliminary experiments; optimal values could vary, thus necessitating further exploration for better efficiency and effectiveness.

Moreover, embeddings, even after feature selection, remain less interpretable compared to raw features, particularly in sensitive, high-stakes applications. Developing methods to enhance interpretability is crucial. Embeddings can also amplify biases in noisy or inconsistently encoded datasets. For low-diversity datasets, there exists the risk of embedding degeneration, limiting the ability to distinguish between classes or relevant groups in an unbiased way.

Embeddings may also add unnecessary complexity in structured tabular data with minimal contextual information, where their informative value is limited, as seen in some of the datasets used in this study. Future work could further investigate the expected use-case and dataset-specific value of embedding-derived features.

6.3 Future Research Directions

In alignment with the above limitations, we see high potential for research that focuses on the following areas: The development of use-case-specific embedding strategies for structured data, boosting the semantic relevance of embedding-derived features, could be highly impactful. Additionally, adaptive feature-weighting and regularization methods could be integrated to enhance robustness and prevent embedding degeneration in complex datasets or datasets with limited representativeness of features or classes.

Improving the interpretability of embeddings is a promising avenue for future research, particularly in privacy-sensitive, high-stakes applications, by developing transparency and privacy-preserving frameworks for structured data. To reduce computational overhead, embedding alternatives could be explored alongside automated, early dimensionality reduction techniques to optimize component selection. This could be combined with feature selection strategies that combine feature importance scores across multiple classifiers and XAI techniques to ensure consistent identification of valuable features and improve model robustness and reliability.

7 Conclusion

Our findings reveal that embedding-based feature enrichment offers performance benefits for ensemble classifiers, especially for datasets with limited feature diversity or class representation. These gains can be further amplified with more advanced ensemble classifiers such as XGBoost or CatBoost. For datasets with comprehensive representation, the performance gains are modest at best, highlighting the selective applicability of this approach. Additionally, embedding-enriched models take full advantage of LLM-derived features, which consistently rank among the most influential in feature importance analysis. Hence, these features may play a critical role in uncovering complex data patterns beyond the reach of the original features.

These insights emphasize the potential of contextual embeddings to advance traditional feature engineering, aligning performance improvements with privacy-preserving strategies. We see high potential for research on optimizing embeddings for structured data, refining dimensionality reduction techniques, and exploring additional pre-trained models and embedding dimensions to further enhance generalizability across a broader range of classification tasks.

References

- [1] Kerkri Abdelmounaim and Mohamed Amine Madani. A hybrid ensemble approach integrating machine learning and deep learning with sentence embeddings for webpage content classification. In *Modern Artificial Intelligence and Data Science 2024: Tools, Techniques and Systems*, pages 85–97. Springer, 2024.
- [2] Sadam Al-Azani and El-Sayed M El-Alfy. Using word embedding and ensemble learning for highly imbalanced data sentiment analysis in short arabic text. *Procedia Computer Science*, 109:359–366, 2017.
- [3] Yoshua Bengio, Aaron Courville, and Pascal Vincent. Representation learning: A review and new perspectives. *IEEE transactions on pattern analysis and machine intelligence*, 35(8):1798–1828, 2013.
- [4] Vadim Borisov, Tobias Leemann, Kathrin Seßler, Johannes Haug, Martin Pawelczyk, and Gjergji Kasneci. Deep neural networks and tabular data: A survey. *IEEE transactions on neural networks and learning systems*, 2022.
- [5] Vadim Borisov, Kathrin Seßler, Tobias Leemann, Martin Pawelczyk, and Gjergji Kasneci. Language models are realistic tabular data generators. In *Proceedings of the International Conference on Learning Representations (ICLR)*, 2023.

- [6] Leo Breiman. Random forests. *Machine Learning*, 45(1):5–32, 2001.
- [7] Tom B Brown, Benjamin Mann, Nick Ryder, Melanie Subbiah, Jared Kaplan, Prafulla Dhariwal, Arvind Neelakantan, Pranav Shyam, Girish Sastry, Amanda Askell, et al. Language models are few-shot learners. *Advances in Neural Information Processing Systems*, 33:1877–1901, 2020.
- [8] Chenjing Cai, Shiwei Wang, Youjun Xu, Weilin Zhang, Ke Tang, Qi Ouyang, Luhua Lai, and Jianfeng Pei. Transfer learning for drug discovery. *Journal of Medicinal Chemistry*, 63(16):8683–8694, 2020.
- [9] Tianqi Chen and Carlos Guestrin. Xgboost: A scalable tree boosting system. In *Proceedings of the 22nd ACM SIGKDD International Conference on Knowledge Discovery and Data Mining*, pages 785–794. ACM, 2016.
- [10] Alexis Cvetkov-Iliev, Alexandre Allauzen, and Gaël Varoquaux. Relational data embeddings for feature enrichment with background information. *Machine Learning*, 112(2):687–720, 2023.
- [11] Jacob Devlin, Ming-Wei Chang, Kenton Lee, and Kristina Toutanova. Bert: Pre-training of deep bidirectional transformers for language understanding. *arXiv preprint arXiv:1810.04805*, 2019.
- [12] Anna Veronika Dorogush, Vasily Ershov, and Andrey Gulin. Catboost: gradient boosting with categorical features support. *arXiv preprint arXiv:1810.11363*, 2018.
- [13] Xi Fang, Weijie Xu, Fiona Anting Tan, Jiani Zhang, Ziqing Hu, Yanjun Jane Qi, Scott Nickleach, Diego Socolinsky, Srinivasan Sengamedu, Christos Faloutsos, et al. Large language models (llms) on tabular data: Prediction, generation, and understanding-a survey. *amazon.science*, 2024.
- [14] Stanislav Fort, Huiyi Hu, and Balaji Lakshminarayanan. Deep ensembles: A loss landscape perspective. *arXiv preprint arXiv:1912.02757*, 2019.
- [15] Jerome H Friedman. Greedy function approximation: A gradient boosting machine. *Annals of Statistics*, 29(5):1189–1232, 2001.
- [16] Jianping Gou et al. Knowledge distillation: A survey. *International Journal of Computer Vision*, 129(6):1789–1819, 2021.
- [17] Asaf Harari and Gilad Katz. Few-shot tabular data enrichment using fine-tuned transformer architectures. In *Proceedings of the 60th Annual Meeting of the Association for Computational Linguistics (Volume 1: Long Papers)*, pages 1577–1591, 2022.
- [18] Xiangnan He, Liqiang Liao, Hanwang Zhang, Liqiang Nie, Xia Hu, and Tat-Seng Chua. Neural collaborative filtering. In *Proceedings of the 26th international conference on world wide web*, pages 173–182, 2017.
- [19] Noah Hollmann, Samuel Müller, Katharina Eggenberger, and Frank Hutter. TabPFN: A transformer that solves small tabular classification problems in a second. *arXiv preprint arXiv:2207.01848*, 2022.

- [20] Sara Hooker, Dumitru Erhan, Pieter-Jan Kindermans, and Been Kim. A benchmark for interpretability methods in deep neural networks. *Advances in Neural Information Processing Systems*, 32, 2019.
- [21] Xin Huang, Ashish Khetan, Milan Cvitkovic, and Zohar Karnin. Tabtransformer: Tabular data modeling using contextual embeddings. In *Advances in Neural Information Processing Systems*, volume 33, pages 8472–8482, 2020.
- [22] Zachary C Lipton. The mythos of model interpretability: In machine learning, the concept of interpretability is both important and slippery. *Queue*, 16(3):31–57, 2018.
- [23] Yinhan Liu, Myle Ott, Naman Goyal, Jingfei Du, Mandar Joshi, Danqi Chen, Omer Levy, Mike Lewis, Luke Zettlemoyer, and Veselin Stoyanov. Roberta: A robustly optimized bert pretraining approach. *arXiv preprint arXiv:1907.11692*, 2019.
- [24] Richard Meyes, Melanie Lu, Constantin Waubert de Puiseau, and Tobias Meisen. Ablation studies in artificial neural networks. *arXiv preprint arXiv:1901.08644*, 2019.
- [25] Shervin Minaee, Nal Kalchbrenner, Erik Cambria, Narjes Nikzad, Meysam Chenaghlu, and Jianfeng Gao. Deep learning–based text classification: a comprehensive review. *ACM computing surveys (CSUR)*, 54(3):1–40, 2021.
- [26] Christoph Molnar. *Interpretable Machine Learning: A Guide for Making Black Box Models Explainable*. 2020.
- [27] Jaehyun Nam, Kyuyoung Kim, Seunghyuk Oh, Jihoon Tack, Jaehyung Kim, and Jinwoo Shin. Optimized feature generation for tabular data via llms with decision tree reasoning. *arXiv preprint arXiv:2406.08527*, 2024.
- [28] Fabian Pedregosa, Gaël Varoquaux, Alexandre Gramfort, Vincent Michel, Bertrand Thirion, Olivier Grisel, Mathieu Blondel, Peter Prettenhofer, Ron Weiss, Vincent Dubourg, Jake Vanderplas, Alexandre Passos, David Cournapeau, Mathieu Brucher, Matthieu Perrot, and Édouard Duchesnay. Scikit-learn: Machine learning in python. *Journal of Machine Learning Research*, 12:2825–2830, 2011.
- [29] Alec Radford, Jeffrey Wu, Rewon Child, David Luan, Dario Amodei, and Ilya Sutskever. Language models are unsupervised multitask learners. OpenAI Blog, 2019.
- [30] Colin Raffel, Noam Shazeer, Adam Roberts, Katherine Lee, Sharan Narang, Michael Matena, Yanqi Zhou, Wei Li, and Peter J Liu. Exploring the limits of transfer learning with a unified text-to-text transformer. *Journal of Machine Learning Research*, 21(140):1–67, 2020.
- [31] Steffen Rendle, Walid Krichene, Li Zhang, and John Anderson. Neural collaborative filtering vs. matrix factorization revisited. In *Proceedings of the 14th ACM Conference on Recommender Systems*, pages 240–248, 2020.
- [32] Qitao Shi, Ya-Lin Zhang, Longfei Li, Xinxing Yang, Meng Li, and Jun Zhou. Safe: Scalable automatic feature engineering framework for industrial tasks. In *2020 IEEE 36th International Conference on Data Engineering (ICDE)*, pages 1645–1656. IEEE, 2020.

- [33] Yuqi Si, Jingqi Wang, Hua Xu, and Kirk Roberts. Enhancing clinical concept extraction with contextual embeddings. *Journal of the American Medical Informatics Association*, 26(11):1297–1304, 2019.
- [34] Chi Sun, Xipeng Qiu, Yige Xu, and Xuanjing Huang. How to fine-tune bert for text classification? In *Chinese computational linguistics: 18th China national conference, CCL 2019, Kunming, China, October 18–20, 2019, proceedings 18*, pages 194–206. Springer, 2019.
- [35] Mukund Sundararajan, Ankur Taly, and Qiqi Yan. Axiomatic attribution for deep networks. In *Proceedings of the 34th International Conference on Machine Learning*, pages 3319–3328, 2017.
- [36] Christina V Theodoris, Ling Xiao, Anant Chopra, Mark D Chaffin, Zeina R Al Sayed, Matthew C Hill, Helene Mantineo, Elizabeth M Brydon, Zexian Zeng, X Shirley Liu, et al. Transfer learning enables predictions in network biology. *Nature*, 618(7965):616–624, 2023.
- [37] Grigorios Tsoumakas, Ioannis Katakis, and Ioannis Vlahavas. Mining multi-label data. *Data mining and knowledge discovery handbook*, pages 667–685, 2010.
- [38] Laurens Van der Maaten and Geoffrey Hinton. Visualizing data using t-sne. *Journal of machine learning research*, 9(11), 2008.
- [39] Ashish Vaswani, Noam Shazeer, Niki Parmar, Jakob Uszkoreit, Llion Jones, Aidan N Gomez, Lukasz Kaiser, and Illia Polosukhin. Attention is all you need. In *Advances in Neural Information Processing Systems*, pages 5998–6008, 2017.
- [40] Zifeng Wang and Jimeng Sun. Transtab: Learning transferable tabular transformers across tables. *Advances in Neural Information Processing Systems*, 35:2902–2915, 2022.
- [41] Thomas Wolf, Lysandre Debut, Victor Sanh, Julien Chaumond, Clement Delangue, Anthony Moi, Pierric Cistac, Tim Rault, et al. Transformers: State-of-the-art natural language processing. In *Proceedings of the 2020 conference on empirical methods in natural language processing: system demonstrations*, pages 38–45, 2020.
- [42] Stephen Wu, Kirk Roberts, Surabhi Datta, Jingcheng Du, Zongcheng Ji, Yuqi Si, Sarvesh Soni, Qiong Wang, Qiang Wei, Yang Xiang, et al. Deep learning in clinical natural language processing: a methodical review. *Journal of the American Medical Informatics Association*, 27(3):457–470, 2020.
- [43] Suping Xu, Xibei Yang, Hualong Yu, Dong-Jun Yu, Jingyu Yang, and Eric CC Tsang. Multi-label learning with label-specific feature reduction. *Knowledge-Based Systems*, 104:52–61, 2016.
- [44] Alice Zheng and Amanda Casari. *Feature engineering for machine learning: principles and techniques for data scientists*. ” O’Reilly Media, Inc.”, 2018.
- [45] Zhi-Hua Zhou and Ji Feng. Deep forest. *National science review*, 6(1):74–86, 2019.

8 Appendix

Table 2: Performance Metrics for Different Feature Subsets Across Datasets and Models

Dataset	Model	Feature Subset	Accuracy	Balanced Accuracy	F1 Score	ROC-AUC
UCI Covertypes	RandomForest	Baseline	0.9021	0.7828	0.9005	0.9884
	RandomForest	GPT2_Selected	0.5722	0.2044	0.5310	0.7567
	RandomForest	RoBERTa_Selected	0.5947	0.2444	0.5602	0.7952
	RandomForest	GPT2_RoBERTa	0.6067	0.2312	0.5677	0.8316
	RandomForest	Baseline_GPT2	0.8469	0.6835	0.8420	0.9801
	RandomForest	Baseline_RoBERTa	0.8464	0.6770	0.8414	0.9793
	RandomForest	Baseline_GPT2_RoBERTa_Selected	0.8153	0.6157	0.8084	0.9729
	XGBoost	Baseline	0.8603	0.7688	0.8590	0.9831
	XGBoost	GPT2_Selected	0.5766	0.2323	0.5454	0.7884
	XGBoost	RoBERTa_Selected	0.5943	0.2639	0.5673	0.8235
	XGBoost	GPT2_RoBERTa	0.6188	0.2984	0.5969	0.8577
	XGBoost	Baseline_GPT2	0.8449	0.7281	0.8429	0.9803
	XGBoost	Baseline_RoBERTa	0.8478	0.7400	0.8459	0.9804
	XGBoost	Baseline_GPT2_RoBERTa_Selected	0.8399	0.7170	0.8377	0.9789
	CatBoost	Baseline	0.8679	0.7653	0.8664	0.9848
	CatBoost	GPT2_Selected	0.5798	0.2391	0.5489	0.8052
	CatBoost	RoBERTa_Selected	0.6001	0.2728	0.5734	0.8331
	CatBoost	GPT2_RoBERTa	0.6271	0.3175	0.6054	0.8699
	CatBoost	Baseline_GPT2	0.8498	0.7251	0.8476	0.9812
	CatBoost	Baseline_RoBERTa	0.8522	0.7367	0.8502	0.9818
CatBoost	Baseline_GPT2_RoBERTa_Selected	0.8456	0.7169	0.8432	0.9801	
UCI Heart Disease	RandomForest	Baseline	0.8167	0.8064	0.8138	0.9175
	RandomForest	GPT2_Selected	0.8333	0.8317	0.8333	0.8917
	RandomForest	RoBERTa_Selected	0.8167	0.8165	0.8169	0.8597
	RandomForest	GPT2_RoBERTa	0.8167	0.8165	0.8169	0.8967
	RandomForest	Baseline_GPT2	0.8000	0.7946	0.7991	0.9063
	RandomForest	Baseline_RoBERTa	0.8167	0.8131	0.8163	0.9226
	RandomForest	Baseline_GPT2_RoBERTa_Selected	0.8333	0.8283	0.8326	0.9220
	XGBoost	Baseline	0.8500	0.8468	0.8497	0.9080
	XGBoost	GPT2_Selected	0.7500	0.7525	0.7506	0.8799
	XGBoost	RoBERTa_Selected	0.7833	0.7828	0.7836	0.8474
	XGBoost	GPT2_RoBERTa	0.7833	0.7795	0.7829	0.9024
	XGBoost	Baseline_GPT2	0.8167	0.8098	0.8153	0.9046
	XGBoost	Baseline_RoBERTa	0.8333	0.8283	0.8326	0.8732
	XGBoost	Baseline_GPT2_RoBERTa_Selected	0.8167	0.8098	0.8153	0.8889
	CatBoost	Baseline	0.8333	0.8283	0.8326	0.9102
	CatBoost	GPT2_Selected	0.8000	0.7980	0.8000	0.8844
	CatBoost	RoBERTa_Selected	0.7833	0.7795	0.7829	0.8642
	CatBoost	GPT2_RoBERTa	0.8500	0.8434	0.8488	0.9046
	CatBoost	Baseline_GPT2	0.8500	0.8434	0.8488	0.9136
	CatBoost	Baseline_RoBERTa	0.8500	0.8434	0.8488	0.9169
CatBoost	Baseline_GPT2_RoBERTa_Selected	0.8500	0.8434	0.8488	0.9158	
UCI Letter Recognition	RandomForest	Baseline	0.9611	0.9608	0.9611	0.9993
	RandomForest	GPT2_Selected	0.4237	0.4240	0.4226	0.8766
	RandomForest	RoBERTa_Selected	0.5917	0.5914	0.5932	0.9405
	RandomForest	GPT2_RoBERTa	0.6591	0.6586	0.6606	0.9569
	RandomForest	Baseline_GPT2	0.9490	0.9485	0.9490	0.9989
	RandomForest	Baseline_RoBERTa	0.9477	0.9473	0.9478	0.9989
	RandomForest	Baseline_GPT2_RoBERTa_Selected	0.9394	0.9391	0.9395	0.9988
	XGBoost	Baseline	0.9591	0.9589	0.9592	0.9996
	XGBoost	GPT2_Selected	0.4015	0.4018	0.4010	0.8846
	XGBoost	RoBERTa_Selected	0.5672	0.5668	0.5696	0.9463
	XGBoost	GPT2_RoBERTa	0.6621	0.6617	0.6635	0.9682
	XGBoost	Baseline_GPT2	0.9424	0.9421	0.9425	0.9992
	XGBoost	Baseline_RoBERTa	0.9427	0.9423	0.9428	0.9992
	XGBoost	Baseline_GPT2_RoBERTa_Selected	0.9343	0.9340	0.9344	0.9990

Continued on next page

Table 2 – continued from previous page

Dataset	Model	Feature Subset	Accuracy	Weighted Accuracy	F1 Score	ROC-AUC
	CatBoost	Baseline	0.9611	0.9608	0.9611	0.9997
	CatBoost	GPT2_Selected	0.4374	0.4374	0.4362	0.9014
	CatBoost	RoBERTa_Selected	0.6010	0.6004	0.6017	0.9555
	CatBoost	GPT2_RoBERTa	0.6995	0.6990	0.7002	0.9752
	CatBoost	Baseline_GPT2	0.9487	0.9484	0.9487	0.9995
	CatBoost	Baseline_RoBERTa	0.9525	0.9522	0.9525	0.9994
	CatBoost	Baseline_GPT2_RoBERTa_Selected	0.9452	0.9448	0.9452	0.9993
UCI Wine Quality	RandomForest	Baseline	0.6751	0.3171	0.6531	0.8588
	RandomForest	GPT2_Selected	0.5552	0.2387	0.5227	0.6793
	RandomForest	RoBERTa_Selected	0.6151	0.2871	0.5925	0.6964
	RandomForest	Baseline_GPT2	0.6751	0.3138	0.6504	0.7651
	RandomForest	Baseline_RoBERTa	0.6625	0.3030	0.6366	0.8298
	RandomForest	GPT2_RoBERTa	0.6088	0.2660	0.5742	0.6988
	RandomForest	Baseline_GPT2_RoBERTa_Selected	0.6972	0.3136	0.6654	0.7384
	XGBoost	Baseline	0.6688	0.3385	0.6544	0.8582
	XGBoost	GPT2_Selected	0.5647	0.2546	0.5436	0.7122
	XGBoost	RoBERTa_Selected	0.5678	0.2590	0.5485	0.7030
	XGBoost	Baseline_GPT2	0.6593	0.3634	0.6468	0.7713
	XGBoost	Baseline_RoBERTa	0.6498	0.3037	0.6308	0.8652
	XGBoost	GPT2_RoBERTa	0.5773	0.2627	0.5552	0.7527
	XGBoost	Baseline_GPT2_RoBERTa_Selected	0.7035	0.3466	0.6832	0.8186
	CatBoost	Baseline	0.6940	0.3365	0.6744	0.8639
	CatBoost	GPT2_Selected	0.5741	0.2552	0.5491	0.6735
	CatBoost	RoBERTa_Selected	0.5678	0.2655	0.5466	0.7326
	CatBoost	Baseline_GPT2	0.6656	0.3188	0.6459	0.8166
	CatBoost	Baseline_RoBERTa	0.6593	0.3107	0.6393	0.8524
	CatBoost	GPT2_RoBERTa	0.5994	0.2805	0.5775	0.7601
CatBoost	Baseline_GPT2_RoBERTa_Selected	0.6593	0.3073	0.6357	0.8546	
UCI Adult	RandomForest	Baseline	0.8560	0.7765	0.8518	0.9089
	RandomForest	GPT2_Selected	0.8291	0.7157	0.8184	0.8702
	RandomForest	RoBERTa_Selected	0.8239	0.7070	0.8124	0.8693
	RandomForest	Baseline_GPT2	0.8594	0.7686	0.8529	0.9119
	RandomForest	Baseline_RoBERTa	0.8604	0.7690	0.8538	0.9112
	RandomForest	GPT2_RoBERTa	0.8347	0.7240	0.8244	0.8806
	RandomForest	Baseline_GPT2_RoBERTa_Selected	0.8593	0.7641	0.8519	0.9095
	XGBoost	Baseline	0.8752	0.8027	0.8716	0.9320
	XGBoost	GPT2_Selected	0.8304	0.7309	0.8231	0.8688
	XGBoost	RoBERTa_Selected	0.8226	0.7230	0.8156	0.8676
	XGBoost	Baseline_GPT2	0.8727	0.8011	0.8693	0.9282
	XGBoost	Baseline_RoBERTa	0.8719	0.8009	0.8687	0.9290
	XGBoost	GPT2_RoBERTa	0.8299	0.7389	0.8246	0.8770
	XGBoost	Baseline_GPT2_RoBERTa_Selected	0.8659	0.7905	0.8621	0.9256
	CatBoost	Baseline	0.8753	0.8024	0.8716	0.9327
	CatBoost	GPT2_Selected	0.8378	0.7387	0.8303	0.8775
	CatBoost	RoBERTa_Selected	0.8320	0.7289	0.8238	0.8760
	CatBoost	Baseline_GPT2	0.8733	0.7966	0.8691	0.9310
	CatBoost	Baseline_RoBERTa	0.8733	0.7975	0.8692	0.9307
	CatBoost	GPT2_RoBERTa	0.8377	0.7447	0.8316	0.8867
CatBoost	Baseline_GPT2_RoBERTa_Selected	0.8724	0.7957	0.8682	0.9302	
Car Evaluation	RandomForest	Baseline	0.9064	0.7784	0.9030	0.9800
	RandomForest	GPT2_Selected	0.7749	0.4937	0.7411	0.9313
	RandomForest	RoBERTa_Selected	0.8099	0.5356	0.7793	0.9525
	RandomForest	Baseline_GPT2_Selected	0.8743	0.6762	0.8655	0.9822
	RandomForest	Baseline_RoBERTa_Selected	0.8830	0.7021	0.8750	0.9849
	RandomForest	GPT2_RoBERTa_Selected	0.8275	0.5668	0.8019	0.9641
	RandomForest	Baseline_GPT2_RoBERTa_Selected	0.8655	0.6641	0.8534	0.9861
	XGBoost	Baseline	0.9883	0.9572	0.9882	0.9983
	XGBoost	GPT2_Selected	0.7895	0.5804	0.7776	0.9244
	XGBoost	RoBERTa_Selected	0.8333	0.5732	0.8182	0.9525
	XGBoost	Baseline_GPT2_Selected	0.9240	0.7890	0.9249	0.9904
	XGBoost	Baseline_RoBERTa_Selected	0.9211	0.7630	0.9193	0.9879

Continued on next page

Table 2 – continued from previous page

Dataset	Model	Feature Subset	Accuracy	Weighted Accuracy	F1 Score	ROC-AUC
	XGBoost	GPT2_RoBERTa_Selected	0.8684	0.6423	0.8609	0.9719
	XGBoost	Baseline_GPT2_RoBERTa_Selected	0.9211	0.7493	0.9207	0.9888
	CatBoost	Baseline	0.9795	0.9496	0.9794	0.9974
	CatBoost	GPT2_Selected	0.8158	0.6192	0.8057	0.9409
	CatBoost	RoBERTa_Selected	0.8450	0.6092	0.8291	0.9604
	CatBoost	Baseline_GPT2_Selected	0.9415	0.8339	0.9420	0.9929
	CatBoost	Baseline_RoBERTa_Selected	0.9415	0.7952	0.9395	0.9903
	CatBoost	GPT2_RoBERTa_Selected	0.8918	0.7052	0.8847	0.9803
	CatBoost	Baseline_GPT2_RoBERTa_Selected	0.9240	0.7959	0.9237	0.9916
Pima Indians Diabetes	RandomForest	Baseline	0.7632	0.7130	0.7548	0.8408
	RandomForest	GPT2_Selected	0.7039	0.6237	0.6783	0.7252
	RandomForest	RoBERTa_Selected	0.7105	0.6375	0.6901	0.6772
	RandomForest	Baseline_GPT2	0.7171	0.6426	0.6957	0.8334
	RandomForest	Baseline_RoBERTa	0.7566	0.6816	0.7355	0.8345
	RandomForest	GPT2_RoBERTa	0.6711	0.5809	0.6367	0.7300
	RandomForest	Baseline_GPT2_RoBERTa_Selected	0.7368	0.6621	0.7155	0.8174
	XGBoost	Baseline	0.7237	0.6827	0.7195	0.8094
	XGBoost	GPT2_Selected	0.7039	0.6544	0.6966	0.7263
	XGBoost	RoBERTa_Selected	0.6382	0.5688	0.6211	0.6387
	XGBoost	Baseline_GPT2	0.7237	0.6783	0.7178	0.8010
	XGBoost	Baseline_RoBERTa	0.7171	0.6557	0.7038	0.8140
	XGBoost	GPT2_RoBERTa	0.6447	0.5739	0.6264	0.7134
	XGBoost	Baseline_GPT2_RoBERTa_Selected	0.7434	0.6891	0.7334	0.8311
	CatBoost	Baseline	0.7632	0.7130	0.7548	0.8557
	CatBoost	GPT2_Selected	0.6974	0.6230	0.6761	0.7305
	CatBoost	RoBERTa_Selected	0.6842	0.6085	0.6620	0.6770
	CatBoost	Baseline_GPT2	0.7632	0.7130	0.7548	0.8306
CatBoost	Baseline_RoBERTa	0.7566	0.6992	0.7451	0.8458	
CatBoost	GPT2_RoBERTa	0.6711	0.5984	0.6511	0.7374	
CatBoost	Baseline_GPT2_RoBERTa_Selected	0.7566	0.6992	0.7451	0.8256	
Titanic	RandomForest	Baseline	0.8531	0.8392	0.8522	0.8855
	RandomForest	GPT2_Selected	0.7966	0.7823	0.7960	0.8528
	RandomForest	RoBERTa_Selected	0.8023	0.7841	0.8007	0.8774
	RandomForest	Baseline_GPT2	0.8475	0.8264	0.8451	0.8741
	RandomForest	Baseline_RoBERTa	0.8362	0.8283	0.8364	0.8853
	RandomForest	GPT2_RoBERTa	0.8192	0.8062	0.8187	0.8610
	RandomForest	Baseline_GPT2_RoBERTa_Selected	0.8305	0.8098	0.8282	0.8741
	XGBoost	Baseline	0.8475	0.8347	0.8468	0.8716
	XGBoost	GPT2_Selected	0.8192	0.8007	0.8175	0.8548
	XGBoost	RoBERTa_Selected	0.8079	0.7998	0.8084	0.8601
	XGBoost	GPT2_RoBERTa	0.8249	0.8108	0.8241	0.8621
	XGBoost	Baseline_GPT2	0.8249	0.8246	0.8262	0.8736
	XGBoost	Baseline_RoBERTa	0.8249	0.8135	0.8246	0.8739
	XGBoost	GPT2_RoBERTa	0.8249	0.8163	0.8251	0.8587
	CatBoost	Baseline	0.8249	0.7997	0.8214	0.8837
	CatBoost	GPT2_Selected	0.8305	0.8126	0.8289	0.8559
	CatBoost	RoBERTa_Selected	0.8249	0.8163	0.8251	0.8826
	CatBoost	Baseline_GPT2	0.8475	0.8291	0.8457	0.8627
CatBoost	Baseline_RoBERTa	0.8418	0.8328	0.8418	0.8944	
CatBoost	GPT2_RoBERTa	0.8362	0.8255	0.8359	0.8753	
CatBoost	Baseline_GPT2_RoBERTa_Selected	0.8418	0.8301	0.8413	0.8797	

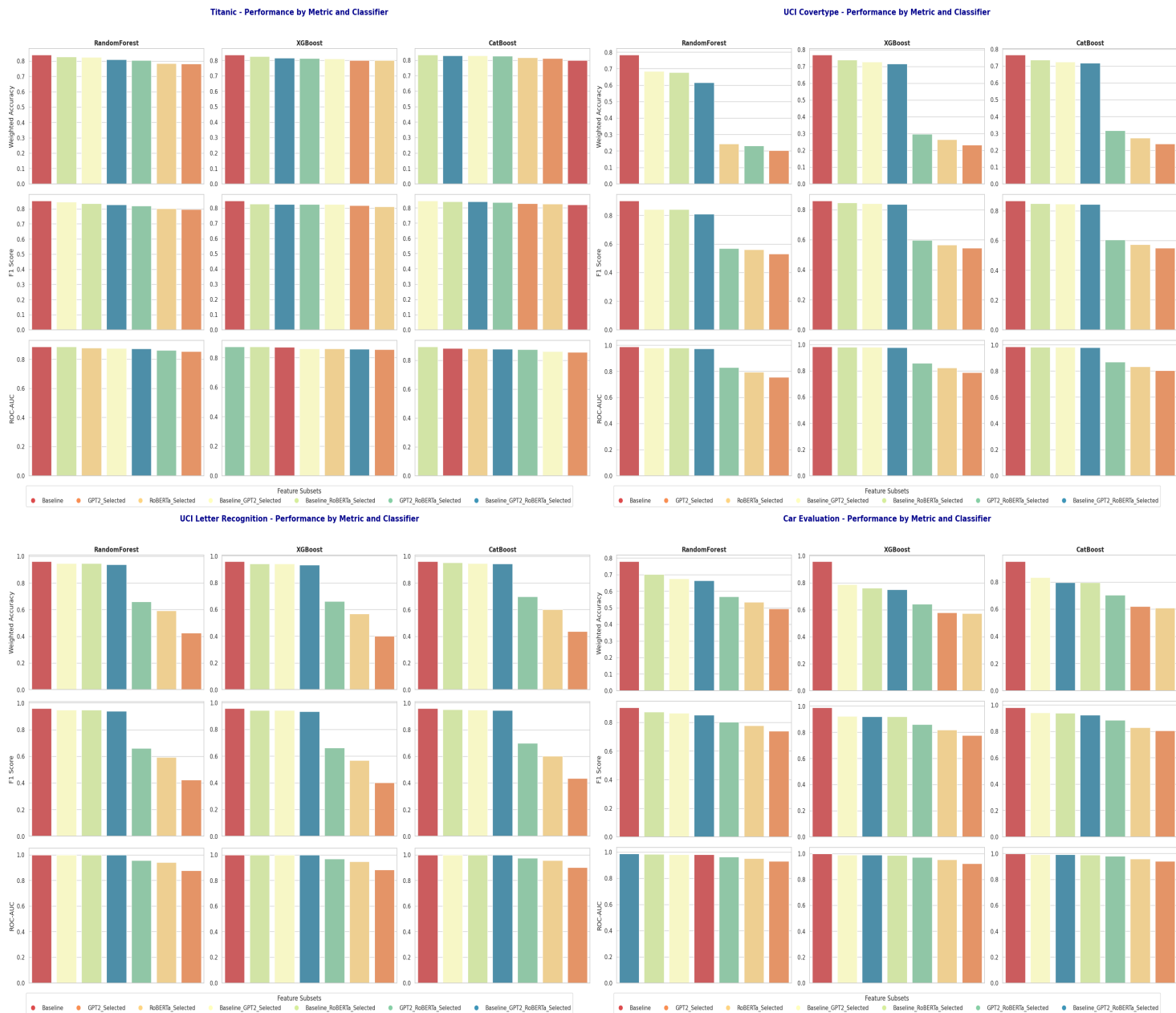
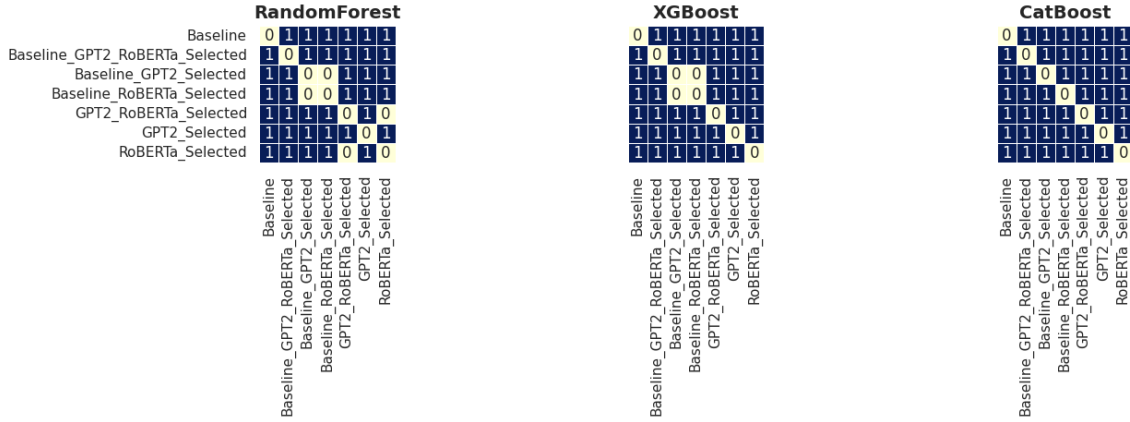
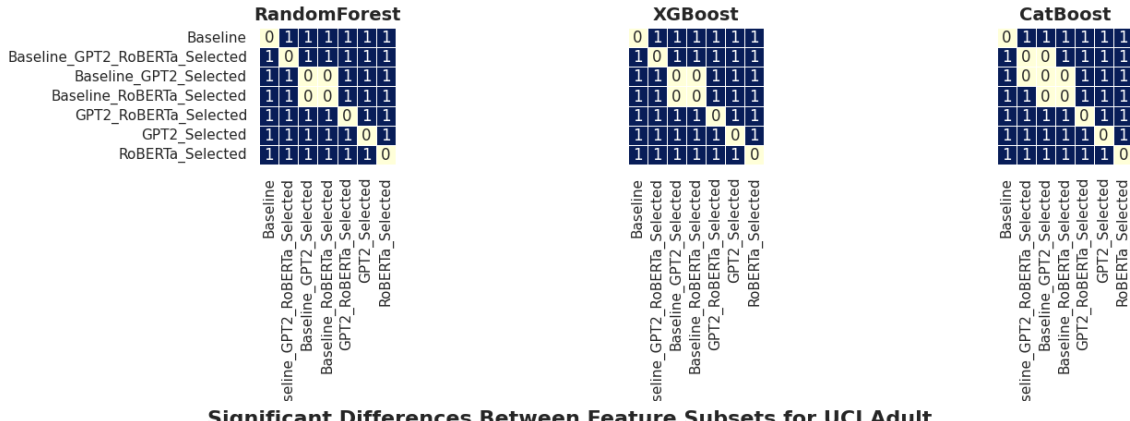


Figure 9: Performance metrics (Weighted/Balanced Accuracy, F1 Score, and ROC-AUC) for different feature subsets on multiple datasets (Titanic, UCI Covertypes, UCI Letter Recognition, and Car Evaluation) using Random Forest, XGBoost, and CatBoost classifiers. The plots show how different feature subsets influence classifier performance, with results sorted by feature subset to facilitate comparisons.

Significant Differences Between Feature Subsets for UCI Covertype



Significant Differences Between Feature Subsets for UCI Letter Recognition



Significant Differences Between Feature Subsets for UCI Adult

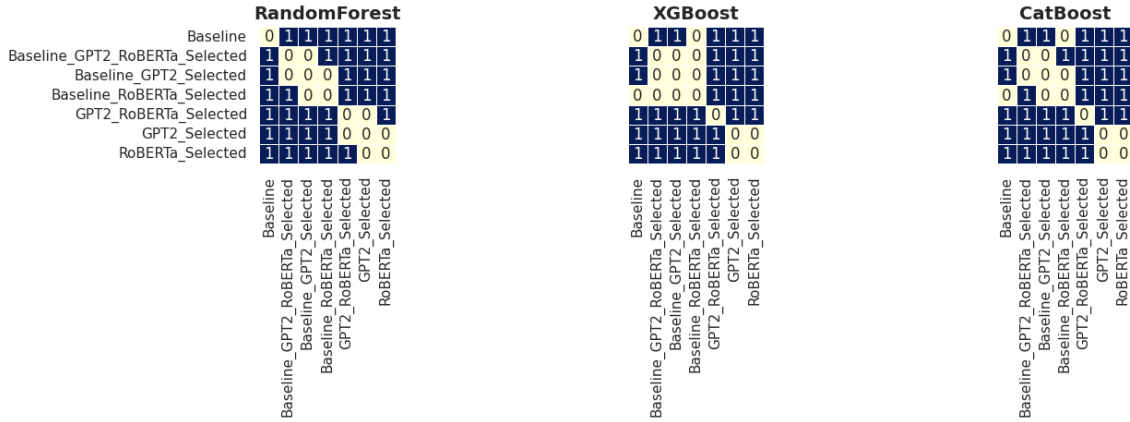
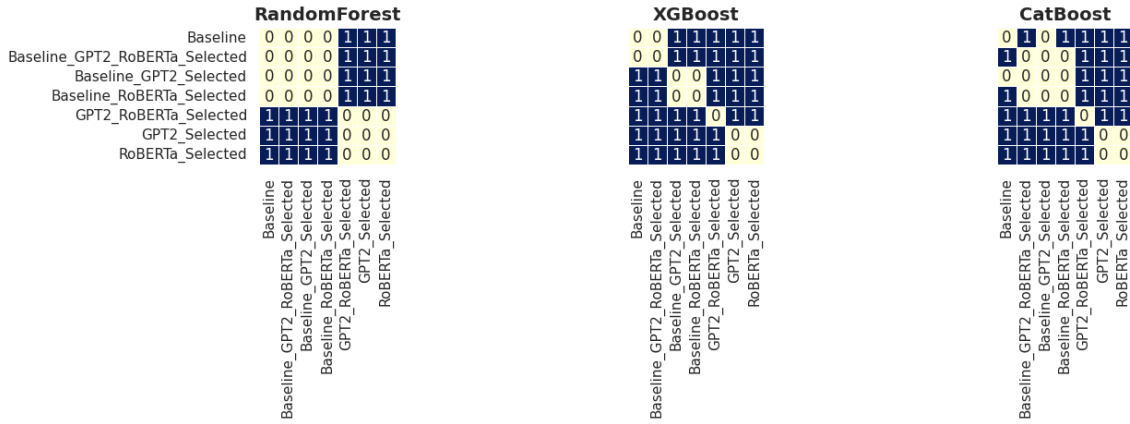
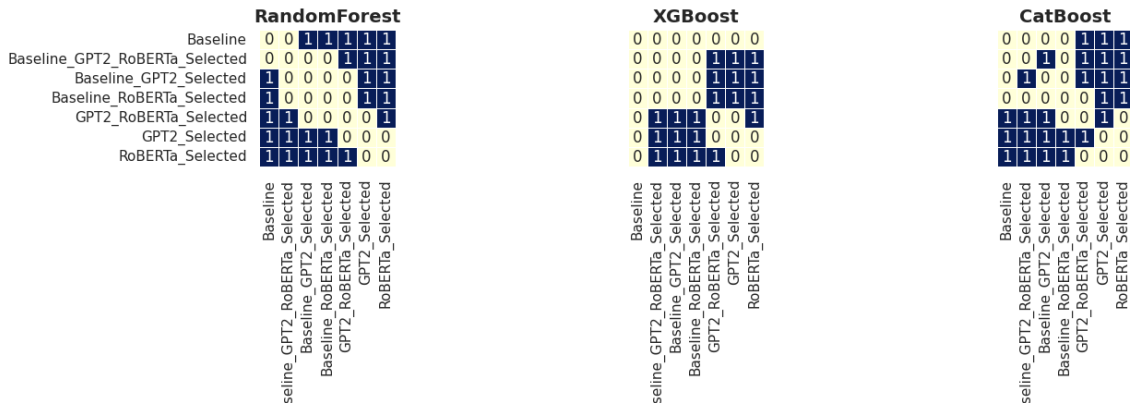


Figure 10: Significant differences between feature subsets across the datasets UCI Covertype, UCI Letter Recognition, and UCI Adult. Each subplot shows pairwise statistical significance tests, where dark cells (value 1) indicate statistically significant differences between feature subsets. The results demonstrate how embeddings (e.g., GPT2, RoBERTa) impact model performance differently across datasets and classifiers.

Significant Differences Between Feature Subsets for Car Evaluation



Significant Differences Between Feature Subsets for Pima Indians Diabetes



Significant Differences Between Feature Subsets for UCI Wine Quality

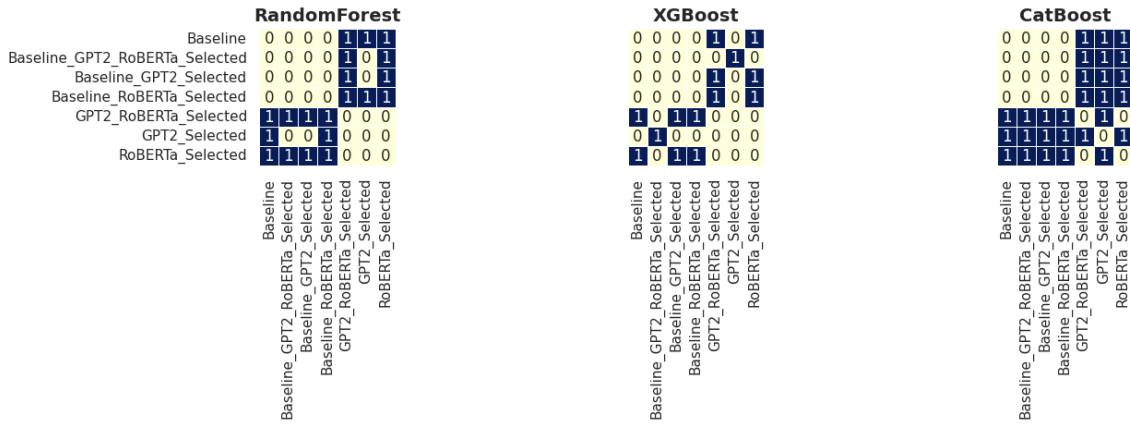
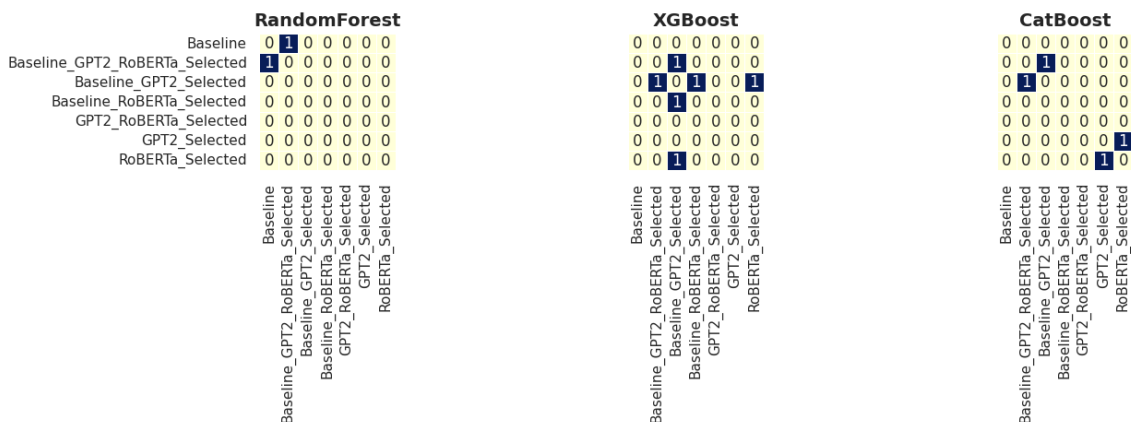


Figure 11: Significant differences between feature subsets across the datasets Car Evaluation, Pima Indians Diabetes, and UCI Wine Quality. Each subplot shows pairwise statistical significance tests, where dark cells (1) indicate statistically significant differences between feature subsets. The results demonstrate how embeddings (e.g., GPT2, RoBERTa) impact model performance differently across datasets and classifiers.

Significant Differences Between Feature Subsets for Titanic



Significant Differences Between Feature Subsets for UCI Heart Disease

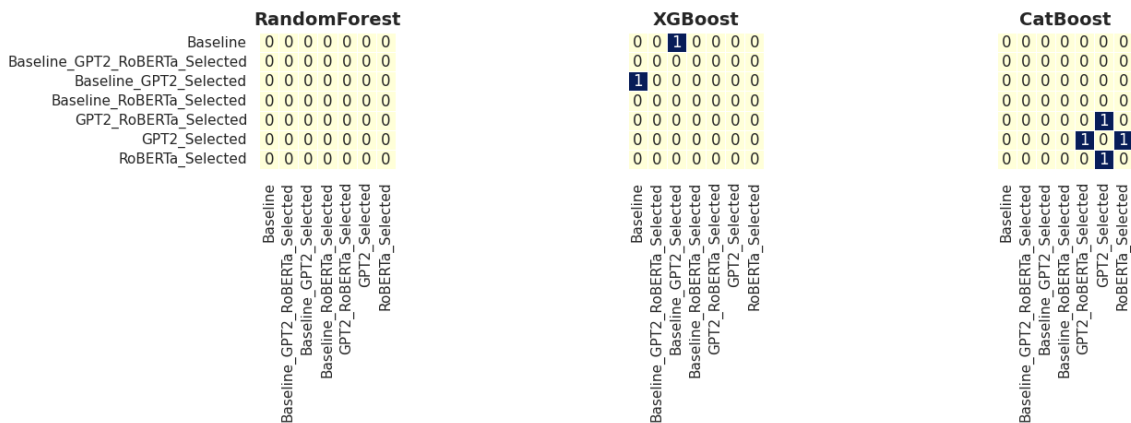


Figure 12: Significant differences between feature subsets across the datasets Titanic and UCI Heart Disease. Each subplot shows pairwise statistical significance tests, where dark cells (1) indicate statistically significant differences between feature subsets. The results demonstrate how embeddings (e.g., GPT2, RoBERTa) impact model performance differently across datasets and classifiers.